

# Theoretical bound of the efficiency of learning with coarse-graining

Minghao Li, Shihao Xia, Youlin Wang, Minglong Lv, and Shanhe Su\*

*Department of Physics, Xiamen University, Xiamen, 361005, People's Republic of China*

(Dated: May 31, 2023)

A thermodynamic formalism describing the efficiency of information learning is proposed, which is applicable for stochastic thermodynamic systems with multiple internal degree of freedom. The learning rate, entropy production rate (EPR), and entropy flow from the system to the environment under coarse-grained dynamics are derived. The Cauchy-Schwarz inequality has been applied to demonstrate the lower bound on the EPR of an internal state. The inequality of EPR is tighter than the Clausius inequality, leading to the derivative of the upper bound on the efficiency of learning. The results are verified in cellular networks with information processes.

## I. INTRODUCTION

Thermodynamic inequalities and uncertainties have a wide range of applications in many fields [1–3]. In this field, the role of information in thermodynamics are currently an active research topic. The Landauer principle has stated that information erasure requires heat dissipation [4], which has been experimentally verified [5, 6]. Markov approximation of the dynamics provides a versatile tool for characterizing information in stochastic thermodynamic systems [7–11]. The efficiency of information exchange was defined as the information transfer over the total entropy production for a pair of Brownian particles [12]. A rate of conditional Shannon entropy reduction describing the learning of the internal process about the external process has been proved to be bounded by the thermodynamic entropy production [13–15].

Despite progresses in informational thermodynamics, one of the unresolved questions is whether a fundamental bound of irreversible entropy production exists in thermodynamic process involving information. Providing this relationship would be beneficial for a better understanding of the trade-off between the learning rate and the energy dissipation.

In this work, the lower limit of the irreversible entropy production rate of thermodynamic systems with multiple internal degrees of freedom will be demonstrated and be applied to reveal the learning efficiency for cellular networks. The contents are organized as follows: In Section II, by using the Markovian master equation under coarse graining and the Cauchy–Schwarz inequality, an inequality associated with the entropy flow from the system to the environment and the entropy production rate is derived. A tighter upper bound for the learning efficiency for one of the internal state is then obtained. In Section III, through a single receptor model and an adaptive cellular network, the learning efficiency for the biological information processing and its upper bound could be verified. Finally, we draw our conclusions in Sec. IV.

## II. STOCHASTIC THERMODYNAMICS UNDER COARSE GRAINING AND LEARNING EFFICIENCY

We first briefly introduce the stochastic thermodynamics of information processing system inspired by the *Escherichia coli* sensory network. The evolution of the system is modeled by the Markovian master equation

$$\dot{p}(y, x) = \sum_{x', y'} \left[ w_{x'y'}^{y'y} p(y', x') - w_{xx'}^{yy'} p(y, x) \right] \quad (1)$$

where  $p(y, x)$  is the probability of the system being in the discrete state  $(y, x)$ ,  $x$  is an external state unaffected by the internal state  $y$ ,  $w_{x'y'}^{y'y}$  represents the transition rate from state  $(y', x')$  to state  $(y, x)$ . Note that the overdot notation in this work is used to emphasize that the quantity is a rate. Assuming that the external and internal states never jump simultaneously,  $w_{x'x}^{y'y}$  is simplified as

$$w_{x'x}^{y'y} = \begin{cases} w_{x'x}^y & x \neq x', y = y' \\ w_{y'y}^x & x = x', y \neq y' \\ 0 & x \neq x', y \neq y' \end{cases} \quad (2)$$

where  $w_{x'x}^y$  is the transition rate of the external state from  $x'$  to  $x$  given that the internal state is  $y$ , and similarly for  $w_{y'y}^x$ .

By considering an internal process comprising two variables  $y = (y_1, y_2)$ , the transition rate  $w_{y'y}^x = w_{(y'_1, y'_2)(y_1, y_2)}^x$ . The internal state  $y_1$  may be indirectly connected to the external state  $x$  via the other internal state  $y_2$ . By using Eqs. (1) and (2), the dynamics of the internal state  $y_1$  given that the external state takes  $x$  is described by the master equation

$$\dot{p}(y_1, x) = \sum_{y_2} \dot{p}(y_1, y_2, x) = \sum_{y'_1} J_{y'_1 y_1}^x, \quad (3)$$

where the marginal probability  $p(y_1, x)$  is obtained by summing  $p(y_1, y_2, x)$  over the variable  $y_2$ ,  $J_{y'_1 y_1}^x =$

\* sushanhe@xmu.edu.cn

$W_{y'_1 y_1}^x p(y'_1, x) - W_{y_1 y'_1}^x p(y_1, x)$ , and

$$W_{y_1 y'_1}^x = \sum_{y_2, y'_2} w_{(y_1, y_2)(y'_1, y'_2)}^x \frac{p(y_1, y_2, x)}{p(y_1, x)} \quad (4)$$

denotes the coarse-grained transition rate from state  $(y_1, x)$  to state  $(y'_1, x)$ .

With the help of Eq. (3), the time derivative of the Shannon entropy  $\dot{S}^{y_1} = -\sum_{y_1} \dot{p}(y_1) \ln p(y_1)$  of the internal state  $y_1$  can be decomposed into three terms [16]

$$\dot{S}^{y_1} = \dot{\sigma}^{y_1} - \dot{S}_r^{y_1} + \dot{I}^{y_1}. \quad (5)$$

$\dot{\sigma}^{y_1}$  and  $\dot{S}_r^{y_1}$  are, respectively, the thermodynamic entropy production rate and the entropy flow from the system to the environment associated with the coarse-grained dynamics of state  $y_1$ , which are defined as

$$\dot{\sigma}^{y_1} = \frac{1}{2} \sum_{y_1, y'_1, x} J_{y'_1 y_1}^x \ln \frac{W_{y'_1 y_1}^x p(y'_1, x)}{W_{y_1 y'_1}^x p(y_1, x)}, \quad (6)$$

and

$$\dot{S}_r^{y_1} = \frac{1}{2} \sum_{y_1, y'_1, x} J_{y'_1 y_1}^x \ln \frac{W_{y'_1 y_1}^x}{W_{y_1 y'_1}^x}. \quad (7)$$

$\dot{\sigma}^{y_1}$  is always positive because of  $W_{y'_1 y_1}^x p(y'_1, x) \geq 0$  and  $J_{y'_1 y_1}^x \ln \frac{W_{y'_1 y_1}^x p(y'_1, x)}{W_{y_1 y'_1}^x p(y_1, x)} \geq 0$  [15].

$$\dot{I}^{y_1} = \frac{1}{2} \sum_{y_1, y'_1, x} J_{y'_1 y_1}^x \ln \frac{p(x|y_1)}{p(x|y'_1)}, \quad (8)$$

quantifies the rate of the coarse-grained internal process  $y_1$  learning about  $x$  with  $p(x|y_1) = \frac{p(x, y_1)}{p(y_1)} = \frac{p(x, y_1)}{\sum_x p(x, y_1)}$  being the conditional probability.

Similar to Eq. (6), the thermodynamic entropy production rate, related to the total internal state  $y = (y_1, y_2)$ , is defined as

$$\dot{\sigma}^y = \frac{1}{2} \sum_{y, y', x} J_{y' y}^x \ln \frac{p(y', x) w_{y' y}^x}{p(y, x) w_{y y'}^x} \quad (9)$$

with  $J_{y' y}^x = w_{y' y}^x p(y', x) - w_{y y'}^x p(y, x)$ . The log-sum inequality  $\sum_i u_i \ln \frac{u_i}{v_i} \geq \sum_i u_i \ln \frac{\sum_i u_i}{\sum_i v_i}$  ( $\forall u_i, v_i \geq 0$ ) [17] implies that

$$\dot{\sigma}^y \geq \dot{\sigma}^{y_1}. \quad (10)$$

This result can also be understood that the process of the change of state  $y_1$  is a part of the internal process.

In the cellular network, when  $\dot{I}^{y_1} \geq 0$ , the cell creates information by perceiving the change of the external state  $x$ . The information learned will be consumed by the cell for driving the internal process. Following Ref. [14, 18, 19], we define an learning efficiency  $\eta^{y_1}$  for biological information processing, which is given by

$$\eta^{y_1} = \frac{\dot{I}^{y_1}}{\dot{S}_r^{y_1}}. \quad (11)$$

Under the condition of steady state, the change rate of the probability  $\dot{p}(y_1, x) = 0$ , leading to the time derivative of the Shannon entropy  $\dot{S}^{y_1} = 0$ . Then, the EPR  $\dot{\sigma}^{y_1} = \dot{S}_r^{y_1} - \dot{I}^{y_1} \geq 0$  indicates that  $\eta^{y_1} = \frac{\dot{I}^{y_1}}{\dot{S}_r^{y_1}} \leq 1$ .

By using the Cauchy-Schwartz inequality  $\sum_i a_i^2 \sum_i b_i^2 \geq (\sum_i a_i b_i)^2$  [20] and the logarithmic inequality  $\frac{(x-y)^2}{x+y} \leq \frac{x-y}{2} \log \frac{x}{y}$  [20], we derive the following inequality associated with  $\dot{S}_r^{y_1}$  and  $\dot{\sigma}^{y_1}$

$$|\dot{S}_r^{y_1}| \leq \sqrt{\theta^{y_1} \dot{\sigma}^{y_1}} \quad (12)$$

where  $\theta^{y_1} = \frac{1}{2} \sum_{y_1, y'_1, x} \left( \ln \frac{W_{y'_1 y_1}^x}{W_{y_1 y'_1}^x} \right)^2 W_{y'_1 y_1}^x p(y'_1, x)$ . In the case of  $\dot{S}_r^{y_1} \geq 0$  and  $\dot{I}^{y_1} \geq 0$ , a tighter upper bound for learning efficiency is obtained, i.e.,

$$\eta^{y_1} = \frac{\dot{I}^{y_1}}{\dot{S}_r^{y_1}} \leq 1 - \frac{\dot{S}_r^{y_1}}{\theta^{y_1}}. \quad (13)$$

This bound, which is the main result of this work, is applicable to plenty of systems as long as the principle of detailed balance is satisfied. In the following section, the above results will be applied to analysis cellular networks. By using the coarse-graining process, the learning efficiency for biological information processing and its upper bound could be determined. The costs and thermodynamic efficiencies for various cellular networks learning about an external random environment will be well characterized.

### III. THE LEARNING EFFICIENCIES OF CELLULAR NETWORKS

#### A. Single receptor model

In the cell, *E. coli* receptors are placed at the membrane and have the ligand-binding site. The kinase is connected to the receptor and its activity depends on the binding of external ligands. The kinase in the active form acts as an enzyme of the phosphorylation reaction of the protein. Here, we consider a single receptor accounting for the indirect regulation of the kinase activity by the binding events. The equivalent eight-state network of the single receptor model is illustrated in Fig. 1(a). Each state of the system is described by  $(a, b, c)$ . The

internal process due to the change of the internal state  $y = (a, b)$  corresponds to a four-state network, as shown in Fig. 1(b). The receptor is occupied by an external ligand at  $b = 1$  or unoccupied at  $b = 0$ . For a given external ligand concentration  $c$ , the free energy difference between the occupied and unoccupied states is given by

$$F(a, 1, c) - F(a, 0, c) = \ln(K_a/c), \quad (14)$$

where  $F(a, b, c)$  represents the free energy of state  $(a, b, c)$ ,  $K_a$  is the dissociation constant,  $\ln K_a$  is associated with a change in the free energy of the receptor, and  $\ln c$  denotes the chemical potential of taking a particle from the solution in a binding event [14]. The subscript in  $K_a$  reflects the interaction between the receptor and the kinase. The activity increases the dissociation constant by considering that  $K_1 > K_0$ . The state of the kinase attached to the receptor may be inactive  $a = 0$  or active  $a = 1$ , resulting in a conformational change in the receptor. The free energy difference between the active and inactive states with fixed values of  $b$  and  $c$  is assumed to be  $\Delta E$ , i.e.,

$$F(1, b, c) - F(0, b, c) = \Delta E. \quad (15)$$

Combining Eqs. (14) with (15), we define the free energy of state  $(a, b, c)$  as

$$F(a, b, c) = a\Delta E + b\ln(K_a/c). \quad (16)$$

The transition rate  $w_{(a,b)(a',b')}^c$  from state  $(a, b, c)$  to state  $(a', b', c)$  given in Fig. 1(b) satisfies the detailed balance condition

$$\ln \left[ w_{(a,b)(a',b')}^c / w_{(a',b')(a,b)}^c \right] = F(a, b, c) - F(a', b', c). \quad (17)$$

In Fig. 1(b),  $\gamma_a$  and  $\gamma_b$  are, respectively, the time-scales of the conformational change and the binding event. The timescale of the binding event is assumed to be much smaller than that of the conformational changes, i.e.,  $\gamma_b \gg \gamma_a$ . In addition to the four-state subsystem in Fig. 1(b), the full model includes the transition of the external ligand concentrations between concentrations  $c_1$  and  $c_2$  at rate  $\gamma_c$  [green dashed arrows in Fig. 1(a)].

By summing out the variable  $b$ , a coarse-grained model with four states is shown by the bottom subfigure in Fig. 1(b). The coarse-grained transition rate from state  $(a, c)$  to  $(a', c)$  under the external ligand concentration  $c$  is given by

$$W_{aa'}^c = \sum_{b,b'} w_{(a,b)(a',b')}^c \frac{p(a, b, c)}{p(a, c)}, \quad (18)$$

where the probability  $p(a, c)$  of coarsened-grained state  $(a, c)$  is calculated by the summation  $\sum_b p(a, b, c)$ . In the limit  $\gamma_a/\gamma_b \rightarrow 0$ , Eq. (18) is simplified as

$$W_{aa'}^c = \sum_{b,b'} w_{(a,b)(a',b')}^c \frac{(c/K_a)^b}{1 + c/K_a} \quad (19)$$

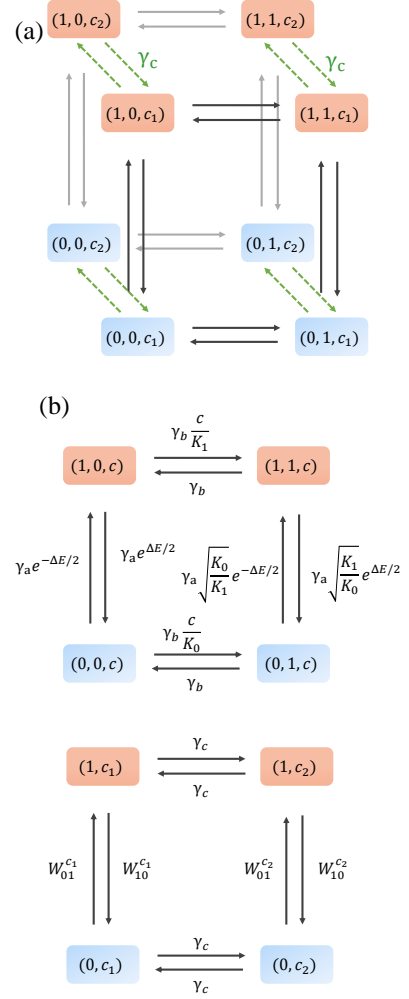


Figure 1. (a) The schematic diagram of the single receptor model. (b) For a given external ligand concentration of  $c$ , the transition rates corresponding to the internal processes (the top subfigure). The schematic diagram of the four-state coarse-graining model by summing out the variable  $b$  (the bottom subfigure).

with  $(c/K_a)^b / (1 + c/K_a)$  corresponding to the stationary condition probability  $p(b|a, c) = \frac{p(a, b, c)}{p(a, c)}$ . The free energy difference between state  $(1, c)$  and state  $(0, c)$  due to the conformational change is then given by

$$F(1, c) - F(0, c) = \ln \frac{W_{10}^c}{W_{01}^c} = \Delta E + \ln \left( \frac{1 + \frac{c}{K_0}}{1 + \frac{c}{K_1}} \right). \quad (20)$$

According to Eqs. (6) and (7) and under the stationarity condition, the entropy production rate associated with the coarse-grained dynamics of state  $a$  is given by

$$\begin{aligned}\dot{\sigma}^a &= \sum_{a,a',c} W_{a'a}^c p(a',c) \ln \frac{W_{a'a}^c p(a',c)}{W_{aa'}^c p(a,c)} \\ &= \dot{S}_r^a - \dot{I}^a,\end{aligned}\quad (21)$$

where the entropy flow from the cell to the environment related to the change of  $a$  reads

$$\dot{S}_r^a = \sum_{a,a',c} W_{a'a}^c p(a',c) \ln \frac{W_{a'a}^c}{W_{aa'}^c}, \quad (22)$$

and the rate of the coarse-grained internal process  $a$  learning about the change of the external ligand concentration  $c$

$$\begin{aligned}\dot{I}^a &= - \sum_{a,a',c} W_{a'a}^c p(a',c) \ln \frac{p(a',c)}{p(a,c)} \\ &= \gamma_c \sum_a [p(a,c_2) - p(a,c_1)] \ln \frac{p(a,c_2)}{p(a,c_1)}.\end{aligned}\quad (23)$$

By applying Eqs. (11)-(13), the efficiency  $\eta^a$  of the dynamics of the kinase in learning about the change of the external ligand concentration

$$\eta^a = \frac{\dot{I}^a}{\dot{S}_r^a} \leq 1 - \frac{\dot{S}_r^a}{\theta^a}, \quad (24)$$

where the coefficient

$$\theta^a = \frac{1}{2} \sum_{a,a',c} \left( \ln \frac{W_{a'a}^c}{W_{aa'}^c} \right)^2 W_{a'a}^c p(a',c). \quad (25)$$

By taking the limit  $\gamma_a/\gamma_b \rightarrow 0$  and using Eq. (19), the entropy flow in (22) is simplified as

$$\dot{S}_r^a = \gamma_c [p(0,c_2) - p(0,c_1)] \ln \left[ \left( \frac{1 + \frac{c_1}{K_0}}{1 + \frac{c_1}{K_1}} \right) \left( \frac{1 + \frac{c_2}{K_1}}{1 + \frac{c_2}{K_0}} \right) \right], \quad (26)$$

and the coefficient in (25) becomes

$$\begin{aligned}\theta^a &= \frac{1}{2} \sum_c \gamma_a \left[ \Delta E + \ln \left( \frac{1 + \frac{c}{K_0}}{1 + \frac{c}{K_1}} \right) \right]^2 \left( 1 + \frac{c}{\sqrt{K_0 K_1}} \right) \\ &\times \left( \frac{e^{\Delta E/2} p(1,c)}{1 + c/K_1} + \frac{e^{-\Delta E/2} p(0,c)}{1 + c/K_0} \right).\end{aligned}\quad (27)$$

Using Eqs. (22)-(27), the learning efficiency  $\eta^a$  varying with  $\gamma_c$  and  $\Delta E$  is plotted in Fig. 2 (a). It is shown that the relation  $\eta^a \leq 1 - \frac{\dot{S}_r^a}{\theta^a}$  always holds, which demonstrates the tightness of the bound in Eq. (24). When  $\Delta E$  is fixed,  $\eta^a$  decreases monotonically with an increase in  $\gamma_c$ . If  $\gamma_c \gg \gamma_a$ , the external concentration jumps too quickly that the intracellular kinase activity couldn't accurately track the change in the external environment,

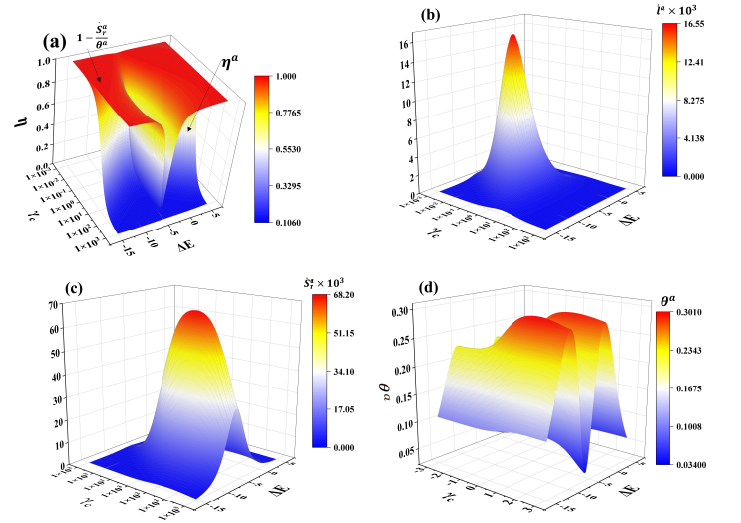


Figure 2. (a) The learning efficiency  $\eta^a$  and the upper limit  $1 - \frac{\dot{S}_r^a}{\theta^a}$  of the single receptor model varying with the transition rate  $\gamma_c$  and the free energy difference  $\Delta E$  between the active and inactive states of CheA. (b) The learning rate  $\dot{I}^a$  varying with  $\gamma_c$  and  $\Delta E$ . (c) The entropy flow  $\dot{S}_r^a$  from the cell to the environment related to the change of  $a$  varying with  $\gamma_c$  and  $\Delta E$ . (d) The coefficient  $\theta^a$  varying with  $\gamma_c$  and  $\Delta E$ . The other parameters  $K_0 = 1/400$ ,  $K_1 = 400$ ,  $\gamma_a = 1$ ,  $\gamma_b = 1000$ ,  $c_1 = 1/3$ , and  $c_2 = 3$ .

leading to the learning rate  $\dot{I}^a \rightarrow 0$  [Fig. 2 (b)]. Consequently,  $\eta^a$  is very small and deviates from the upper bound  $1 - \frac{\dot{S}_r^a}{\theta^a}$ . When  $\Delta E$  is larger than  $-2.2$  or smaller than  $-12.5$ , the entropy flow  $\dot{S}_r^a$  [Fig. 2 (c)] and the coefficient  $\theta^a$  [Fig. 2 (d)] are not very sensitive to the variation of  $\gamma_c$ , such that  $1 - \frac{\dot{S}_r^a}{\theta^a}$  does not change significantly with respect to  $\gamma_c$ . For a  $\Delta E$  between  $-12.5$  and  $-2.2$ , the increase of  $\gamma_c$  results in the dramatic changes in the coefficient  $\theta^a$  [Fig. 2 (d)] and  $1 - \frac{\dot{S}_r^a}{\theta^a}$  [Fig. 2 (a)]. If  $\gamma_c$  is much smaller than  $\gamma_a$ , both the actual efficiency  $\eta^a$  and the upper bound  $1 - \frac{\dot{S}_r^a}{\theta^a}$  approach unity, as the learning rate  $\dot{I}^a$  [Fig. 2 (b)] and the entropy flow  $\dot{S}_r^a$  [Fig. 2 (c)] simultaneously tend to zero.

For a given value of  $\gamma_c$ , the values of the learning efficiency  $\eta^a$  and the upper bound  $1 - \frac{\dot{S}_r^a}{\theta^a}$  first decrease and then increase with the increase of  $\Delta E$  [Fig. 2 (a)]. Compared with  $\eta^a$ ,  $1 - \frac{\dot{S}_r^a}{\theta^a}$  is more sensitive to the change of  $\Delta E$ , because  $\theta^a$  as a function of  $\Delta E$  displays a bimodal structure with large fluctuation [Fig. 2 (d)]. There exists a point of  $\Delta E$  where  $1 - \frac{\dot{S}_r^a}{\theta^a}$  reaches its minimum value close to  $\eta^a$  due to the fact that  $\theta^a$  approaches the lower limit [Fig. 2 (b)] and  $\dot{S}_r^a$  is relatively large [Fig. 2 (c)]. By varying with  $\Delta E$ , Figs. 2(b) and 2(c) indicate that both  $\dot{I}^a$  and  $\dot{S}_r^a$  will have their respective maximum values.

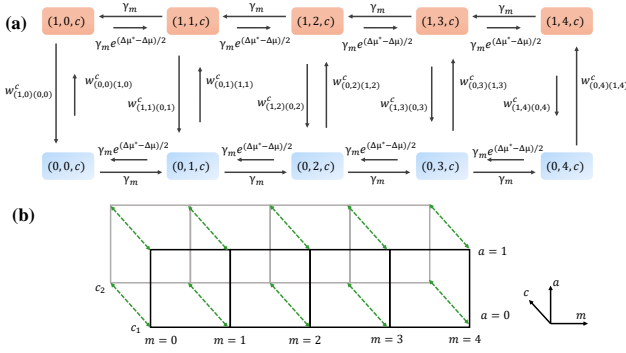


Figure 3. (a) The schematic diagram of the internal process in the adaptive model. (b) The full model containing the jump of the external ligand concentration.

## B. Model with adaptation

Adaptation, in a biological sense, refers to a characteristic of an organism that makes it fit for its environment. We consider an adaptive model (Fig. 3) that incorporates the methylation level  $m$  [14], which is a self-regulation factor for the activity  $a$  of the kinase. In this model, the activity  $a = 1$  if the kinase is active and  $a = 0$  if it is inactive, as shown in Fig. 3. Without the existence of external ligands, the average value of  $a$  is assumed to be equal to  $1/2$ . A change in the external ligand concentration  $c$  quickly changes  $a$  at a time-scale  $\gamma_a^{-1}$ , while the methylation level  $m$  provides the adaption effect by adjusting the average of  $a$  back to  $1/2$  at a time-scale  $\gamma_m^{-1} \gg \gamma_a^{-1}$ . More specifically, a decreasing in  $c$  leads to a fast growth of  $a$ . The change in  $a$  leads to a slow decrease in the methylation level  $m$  which acts back on the activity by slowly reducing  $a$  to  $1/2$ . In the internal process of the cell, the methylation level  $m$  and the kinase activity  $a$  forms a negative feedback network that maintains  $a$  at a stable level.

By considering that the binding event is faster than the conformational change and integrating out the variable  $b$ , the free energy difference between the active state  $(1, m, c)$  and the inactive state  $(0, m, c)$  is obtained from Eq. (20), i.e.,

$$F(1, m, c) - F(0, m, c) = \Delta E(m) + \ln \left( \frac{1 + \frac{c}{K_0}}{1 + \frac{c}{K_1}} \right), \quad (28)$$

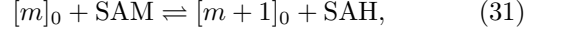
where the energy dependence on the methylation level

$$\Delta E(m) \equiv -\frac{m}{4} \ln \frac{K_1}{K_0}. \quad (29)$$

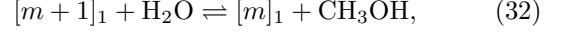
For simplicity, it is assumed that free energy of state  $(a, m, c)$

$$F(a, m, c) = a\Delta E(m) + a \ln \left( \frac{1 + \frac{c}{K_0}}{1 + \frac{c}{K_1}} \right). \quad (30)$$

The methylation level  $m$  is controlled by the chemical reactions. If  $a = 0$ , the receptor may be methylated due to the reaction



where SAM is a shortened form of the S-adenosyl methionine molecule and SAH represents is an abbreviation of the S-adenosyl-L-homocysteine molecule, and the subscript denotes the value of  $a$ . The free energy difference of the reaction is given by  $\mu_{\text{SAM}} - \mu_{\text{SAH}}$ . On the other hand, if  $a = 1$ , the receptor may be demethylated with the reaction



where the free energy difference

$$\begin{aligned} \mu_{\text{H}_2\text{O}} - \mu_{\text{CH}_3\text{OH}} + F(1, m+1, c) - F(1, m, c) \\ = \mu_{\text{H}_2\text{O}} - \mu_{\text{CH}_3\text{OH}} - \frac{1}{4} \ln \frac{K_1}{K_0}. \end{aligned} \quad (33)$$

The chemical potential difference

$$\Delta\mu = \mu_{\text{SAM}} + \mu_{\text{H}_2\text{O}} - \mu_{\text{SAH}} - \mu_{\text{CH}_3\text{OH}}, \quad (34)$$

provides the affinity for driving the internal process.

The variable  $(a, m)$  defines the internal process. The schematic diagram of the internal process in the adaptive model and each transition rate between difference states are shown in Fig. 3 (a). The full model containing the jump of the external ligand concentration with rate  $\gamma_c$  between  $c_1$  and  $c_2$  is presented in Fig. 3 (b).

In Fig. 3 (a), the transition rate  $w_{(1,m)(0,m)}^c$  from the active state  $(1, m, c)$  and the inactive state  $(0, m, c)$  is calculated by Eq. (19), while the only difference is that the energy dependence on the methylation level in Eq. (29) is taken into account. In addition, the transition rates between state  $(1, m, c)$  and state  $(0, m, c)$  is related to the free energy difference in Eq. (28) as

$$F(1, m, c) - F(0, m, c) = \ln \frac{w_{(1,m)(0,m)}^c}{w_{(0,m)(1,m)}^c}. \quad (35)$$

The length of the arrow in Fig. 3 (a) indicates the relative magnitude of  $w_{(1,m)(0,m)}^c$  and  $w_{(0,m)(1,m)}^c$ . The formulas of the transition rates between state  $(a, m, c)$  and state  $(a, m+1, c)$  are presented in Fig. 3 (a), ensuring that the adaptation effects happens if  $\Delta\mu$  overcomes the affinity in the internal cycle  $\Delta\mu^* = \frac{1}{4} \ln \frac{K_1}{K_0}$ . In other words, the increase of  $a$  reduces the methylation level  $m$  which in turn tends to reduce the the value of  $a$ .

By using Eqs. (21)-(23), the coarse-graining entropy production rate  $\dot{\sigma}^a$ , entropy flow  $\dot{S}_r^a$  from cell to environment, and learning rate  $\dot{l}^a$  associated with the change of the internal state  $a$  in the adaptive model can be computed. The only difference is that the coarse-grained transition rate from state  $(a, c)$  to  $(a', c)$  under the external ligand concentration  $c$  is given by

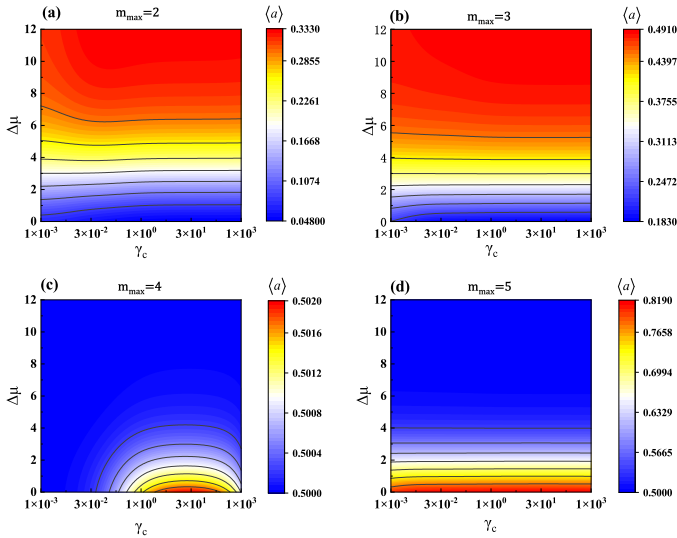


Figure 4. For the maximum methylation level  $m_{max} = 2, 3, 4, 5$ , the average  $\langle a \rangle$  of state  $a$  varying with the transition rate  $\gamma_c$  and the chemical potential difference  $\Delta\mu$ . For the model with adaptation, the parameters  $K_0 = 1/400$ ,  $K_1 = 400$ ,  $\gamma_a = 1$ ,  $\gamma_m = 10^{-2}$ ,  $c_1 = 1/3$ , and  $c_2 = 3$ .

$$W_{aa'}^c = \sum_{m, m'} w_{(a, m)(a', m')}^c \frac{p(a, m, c)}{p(a, c)}, \quad (36)$$

where the probability  $p(a, c)$  of coarsened-grained state  $(a, c)$  is determined by the summation  $\sum_m p(a, m, c)$ . In the same way, the efficiency  $\eta^a$  of the dynamics of the internal state  $a$  in learning about the change of external ligand concentration and its upper limit are computed by Eqs. (24) and (25).

In the adaptive model, the intracellular kinase activity  $a$  will reponse to the change in the external ligand concentration  $c$ . This process is indirectly regulated by altering the methylation level  $m$ . For the maximum methylation level  $m_{max} = 2, 3, 4, 5$ , Fig. 4 plots the average  $\langle a \rangle$  of state  $a$  varying with the transition rate  $\gamma_c$  and the chemical potential difference  $\Delta\mu$ . For a given level of methylation level  $m$ , both  $\gamma_c$  and  $\Delta\mu$  affects the activity of the kinase. When  $m_{max} = 4$ , the average  $\langle a \rangle$  of state  $a$  is more inclined to maintain around  $1/2$  even with large variations of  $\gamma_c$  and  $\Delta\mu$ . That is to say that the feedback network in Fig (3) is capable of maintaining  $a$  at a stable level by optimizing the methylation level  $m$ .

By applying Eqs. (22)-(25) and choosing  $m_{max} = 4$ , Fig. 5 plots the learning efficiency  $\eta^a$  and the upper bound  $1 - \frac{\dot{S}_r^a}{\theta^a}$  for the adaptive model varying with the transition rate  $\gamma_c$  and the chemical potential difference  $\Delta\mu$ . As illustrated in Fig. 5 (a), for a fixed value of  $\Delta\mu$ ,  $\eta^a$  and its upper bound  $1 - \frac{\dot{S}_r^a}{\theta^a}$  decrease monotonically as  $\gamma_c$  increases, while the learning rate  $\dot{a}$ , entropy flow  $\dot{S}_r^a$ , and coefficient  $\theta^a$  appear to be nonmonotonic functions of  $\gamma_c$ . When  $\gamma_c$  is fixed,  $\eta^a$  and  $1 - \frac{\dot{S}_r^a}{\theta^a}$  are not sensitive

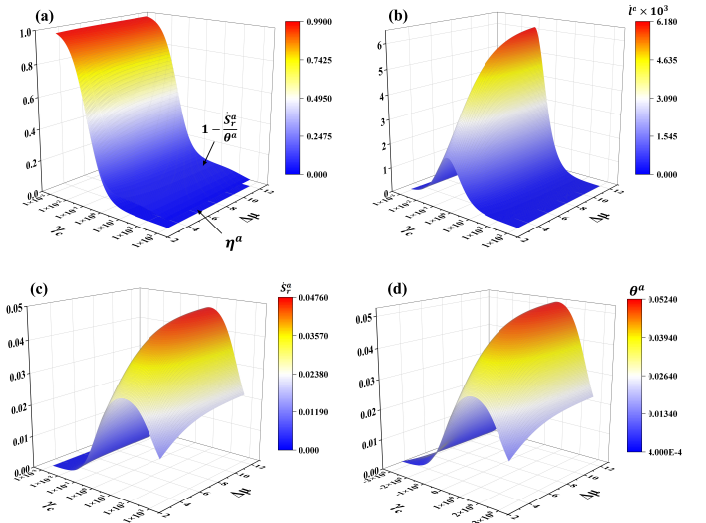


Figure 5. (a) The learning efficiency  $\eta^a$  and the upper limit  $1 - \frac{\dot{S}_r^a}{\theta^a}$  of the model with adaptation varying with the transition rate  $\gamma_c$  and chemical potential difference  $\Delta\mu$ . (b) The learning rate  $\dot{a}$  varying with  $\gamma_c$  and  $\Delta\mu$ . (c) The entropy flow  $\dot{S}_r^a$  from the cell to the environment related to the change of  $a$  varying with  $\gamma_c$  and  $\Delta\mu$ . (d) The coefficient  $\theta^a$  varying with  $\gamma_c$  and  $\Delta\mu$ .

to the change of  $\Delta\mu$ , as  $\dot{a}$ ,  $\dot{S}_r^a$ , and  $\theta^a$  monotonically increase with the increase of  $\Delta\mu$  at the same time. The increase of  $\Delta\mu$  will accelerate the transition rates between different methylation levels, which makes the response of  $m$  to the change in the external concentration  $c$  more sensitive. This enables the internal state  $a$  learning more external information per unit time, but also makes the network also generates more dissipation. It is important to observe that  $\eta^a$  is always smaller than  $1 - \frac{\dot{S}_r^a}{\theta^a}$ , which shows the evidence about the validity of Eq. (24).

#### IV. CONCLUSION

A coarse-graining approach has been developed to quantify the upper bound of the efficiency of learning in multivariable systems, which is tighter than that given by the conventional second law of thermodynamics. By applying this approach to thermodynamic processes in cellular networks, the general applicability of our method has been demonstrated. Our findings have important implications for understanding the fundamental principles governing the dynamics of complex systems.

#### ACKNOWLEDGMENTS

This work has been supported by the National Natural Science Foundation (Grants No. 12075197) and the Fundamental Research Fund for the Central Universities

(No. 20720210024).

- 
- [1] J. Lu, Z. Wang, J. Peng, C. Wang, J.-H. Jiang, and J. Ren, *Physical Review B* **105**, 115428 (2022).
- [2] A. Pal, S. Reuveni, and S. Rahav, *Physical Review Research* **3**, L032034 (2021).
- [3] A. C. Barato and U. Seifert, *Physical review letters* **114**, 158101 (2015).
- [4] R. Landauer, *IBM journal of research and development* **5**, 183 (1961).
- [5] S. Toyabe, T. Sagawa, M. Ueda, E. Muneyuki, and M. Sano, *Nature physics* **6**, 988 (2010).
- [6] A. Bérut, A. Arakelyan, A. Petrosyan, S. Ciliberto, R. Dillenschneider, and E. Lutz, *Nature* **483**, 187 (2012).
- [7] T. R. Gingrich and J. M. Horowitz, *Physical review letters* **119**, 170601 (2017).
- [8] C. W. Lynn, C. M. Holmes, W. Bialek, and D. J. Schwab, *Physical Review E* **106**, 034102 (2022).
- [9] T. R. Gingrich, J. M. Horowitz, N. Perunov, and J. L. England, *Physical review letters* **116**, 120601 (2016).
- [10] C. W. Lynn, C. M. Holmes, W. Bialek, and D. J. Schwab, *Physical review letters* **129**, 118101 (2022).
- [11] Z. Lin, Y. Y. Yang, W. Li, J. Wang, and J. He, *Physical Review E* **101**, 022117 (2020).
- [12] A. E. Allahverdyan, D. Janzing, and G. Mahler, *Journal of Statistical Mechanics: Theory and Experiment* **2009**, P09011 (2009).
- [13] A. Barato, R. Chetrite, A. Faggionato, and D. Gabrielli, *Journal of Statistical Mechanics: Theory and Experiment* **2019**, 084017 (2019).
- [14] A. C. Barato, D. Hartich, and U. Seifert, *New Journal of Physics* **16**, 103024 (2014).
- [15] A. Barato, D. Hartich, and U. Seifert, *Physical Review E* **87**, 042104 (2013).
- [16] S. Su, J. Chen, Y. Wang, J. Chen, and C. Uchiyama, *arXiv preprint arXiv:2209.08096* (2022).
- [17] Y.-Z. Zhen, D. Egloff, K. Modi, and O. Dahlsten, *Physical Review Letters* **127**, 190602 (2021).
- [18] S. Goldt and U. Seifert, *Physical review letters* **118**, 010601 (2017).
- [19] D. Hartich, A. C. Barato, and U. Seifert, *Journal of Statistical Mechanics: Theory and Experiment* **2014**, P02016 (2014).
- [20] N. Shiraishi and K. Saito, *Journal of Statistical Physics* **174**, 433 (2019).
- [21] T. Van Vu and Y. Hasegawa, *Physical Review Letters* **126**, 010601 (2021).
- [22] E. Aurell, C. Mejía-Monasterio, and P. Muratore-Ginanneschi, *Physical review letters* **106**, 250601 (2011).
- [23] P. Pietzonka and U. Seifert, *Physical review letters* **120**, 190602 (2018).
- [24] K. Proesmans, J. Ehrich, and J. Bechhoefer, *Physical Review Letters* **125**, 100602 (2020).
- [25] J. M. Horowitz and M. Esposito, *Physical Review X* **4**, 031015 (2014).
- [26] M. Esposito, *Physical Review E* **85**, 041125 (2012).
- [27] J. M. Horowitz and T. R. Gingrich, *Nature Physics* **16**, 15 (2020).
- [28] B. Ertel, J. van der Meer, and U. Seifert, *Physical Review E* **105**, 044113 (2022).
- [29] C. Van den Broeck and M. Esposito, *Physica A: Statistical Mechanics and its Applications* **418**, 6 (2015).
- [30] U. Seifert, *Reports on progress in physics* **75**, 126001 (2012).
- [31] C. Jarzynski, *Annu. Rev. Condens. Matter Phys.* **2**, 329 (2011).
- [32] A. Murugan, D. A. Huse, and S. Leibler, *Proceedings of the National Academy of Sciences* **109**, 12034 (2012).
- [33] M. Skoge, S. Naqvi, Y. Meir, and N. S. Wingreen, *Physical review letters* **110**, 248102 (2013).
- [34] A. H. Lang, C. K. Fisher, T. Mora, and P. Mehta, *Physical review letters* **113**, 148103 (2014).
- [35] Y. Hasegawa and T. Van Vu, *Physical Review E* **99**, 062126 (2019).
- [36] A. M. Timpanaro, G. Guarnieri, J. Goold, and G. T. Landi, *Physical review letters* **123**, 090604 (2019).
- [37] K. Proesmans and J. M. Horowitz, *Journal of Statistical Mechanics: Theory and Experiment* **2019**, 054005 (2019).
- [38] L. Yan, T. Xiong, K. Rehan, F. Zhou, D. Liang, L. Chen, J. Zhang, W. Yang, Z. Ma, and M. Feng, *Physical review letters* **120**, 210601 (2018).
- [39] D. Chiuchì and S. Pigolotti, *Physical Review E* **97**, 032109 (2018).
- [40] J. Guo, J. Wang, Y. Wang, and J. Chen, *Physical Review E* **87**, 012133 (2013).
- [41] J. Guo, J. Wang, Y. Wang, and J. Chen, *Journal of Applied Physics* **113**, 143510 (2013).
- [42] J. He, J. Chen, and B. Hua, *Physical Review E* **65**, 036145 (2002).
- [43] C. Li, Y. Zhang, J. Wang, and J. He, *Physical Review E* **88**, 062120 (2013).
- [44] J.-H. Jiang, *Physical Review E* **90**, 042126 (2014).